Performance Evaluation of Train Moving-Block Control

Giovanni Neglia, Sara Alouf, Abdulhalim Dandoush, Sebastien Simoens, Pierre Dersin, Alina Tuholukova, Jérôme Billion, Pascal Derouet

Performance Evaluation of Train Moving-Block Control

Giovanni Neglia, Sara Alouf, Abdulhalim Dandoush, Sebastien Simoens , Pierre Dersin , Alina Tuholukova, Jérôme Billion, Pascal Derouet

RESEARCH REPORT

N° 8917

May 2016

Project-Team Maestro

ISSN 0249-6399 ISRN INRIA/RR--8917--FR+ENG

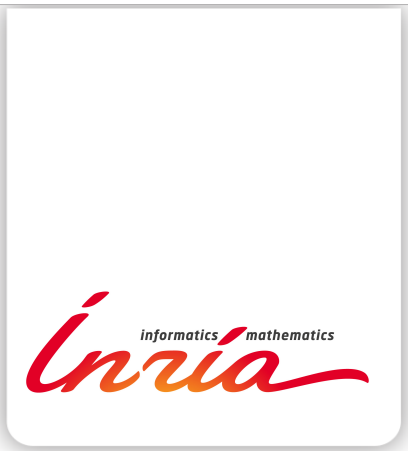

Performance Evaluation of Train Moving-Block Control

Giovanni Neglia*, Sara Alouf*, Abdulhalim Dandoush†,
Sebastien Simoens ‡, Pierre Dersin ‡, Alina Tuholukova*,
Jérôme Billion‡, Pascal Derouet‡

Project-Team Maestro

Research Report n° 8917 — May 2016 — 28 pages

Abstract: In moving block systems for railway transportation a central controller periodically communicates to the train how far it can safely advance. On-board automatic protection mechanisms stop the train if no message is received during a given time window.
In this report we consider as reference a typical implementation of moving-block control for metro and quantify the rate of spurious Emergency Brakes (EBs), i.e. of train stops due to communication losses and not to an actual risk of collision. Such unexpected EBs can happen at any point on the track and are a major service disturbance.
Our general formula for the EB rate requires a probabilistic characterization of losses and delays. We derive an exact formula for the case of homogeneous and independent packet losses and we use the results of this analysis to design an efficient Monte Carlo method that takes into account correlated losses due to handovers. We validate our approach via discrete-event simulations, including simulations with ns-3 for which we have developed additional modules for train systems. Our approach is computationally efficient even when emergency brakes are very rare (as they should be) and can no longer be estimated via discrete-event simulations.

Key-words: Emergency brakes, Communication Based Train Control (CBTC), European Rail Traffic Management System (ERTMS), European Train Control System (ETCS), Monte Carlo Method.

* Inria Sophia Antipolis-Méditerranée, firstname.familyname@inria.fr
† ESME Sudria, dandoush@esme.fr
‡ Alstom Transport, firstname.secondname@transport.alstom.com

RESEARCH CENTRE
SOPHIA ANTIPOLIS – MÉDITERRANÉE

2004 route des Lucioles - BP 93
06902 Sophia Antipolis Cedex

Evaluation de Performance du Contrôle de Train à Canton Glissant

Résumé : Le contrôle du trafic ferroviaire repose sur le principe de base qu'à tout instant au plus un train peut occuper un tronçon de la voie ferrée. Traditionnellement, ces tronçons (ou cantons) sont fixes. Dans les systèmes à canton glissant, un ordinateur central à chaque zone détermine les cantons propres à cette zone. Tous les trains d'une zone doivent périodiquement communiquer à l'ordinateur central leurs positions actuelles, celui-ci peut alors calculer les limites à ne pas dépasser pour chaque train. L'information relative à chaque train lui est alors transmise par voie radio. Le contrôle à canton glissant permet une meilleure exploitation de la voie ferrée tout en réduisant le cout des équipements le long des rails. Ce type de contrôle est utilisé dans le système *Communication Based Train Control* (CBTC) qu'on trouve dans les transports en commun ferrés et est à l'étude pour la nouvelle génération du *European Train Control System* pour les trains à grande vitesse. On considère le cas où la communication entre trains et équipements au sol se fait par ondes radio. Des mécanismes de protection à bord du train déclenchent un freinage d'urgence si aucun message de contrôle n'est reçu par le train pendant un certain temps prédéterminé. Ce type de freinage d'urgence, intempestif, est une source majeure de perturbation pour le trafic ferroviaire et il est essentiel de bien dimensionner le système de communication afin de limiter les freinages d'urgences intempestifs. Dans ce rapport, nous étudions le contrôle ferroviaire à canton glissant et considérons comme cas d'étude des lignes de métro déployées par Alstom Transport, un acteur majeur du monde ferroviaire. En particulier, nous quantifions le taux de freinages d'urgence intempestifs (les freinages dus aux erreurs de communications radio et non pas à un réel risque de collision). Nous obtenons une formule exacte lorsque les pertes de paquets sont homogènes et indépendantes et exploitons cette formule pour concevoir une méthode Monte-Carlo permettant de calculer le taux de freinages d'urgence intempestifs lorsque les pertes de paquets sont aussi dues aux phases de handover dans la communication sans-fil. Nous validons notre approche par des simulations à événements discrets. Nous utilisons en particulier le simulateur ns-3 pour lequel nous avons implanté des modules supplémentaires nécessaires à la simulation des systèmes ferroviaires. Notre approche est efficace même lorsque les freinages d'urgence intempestifs sont extrêmement rares (comme ils devraient l'être) alors qu'une simulation à événements discrets ne serait plus envisageable.

Mots-clés : Freinages d'urgence intempestifs, Communication Based Train Control (CBTC), European Rail Traffic Management System (ERTMS), European Train Control System (ETCS), Méthode de Monte-Carlo.

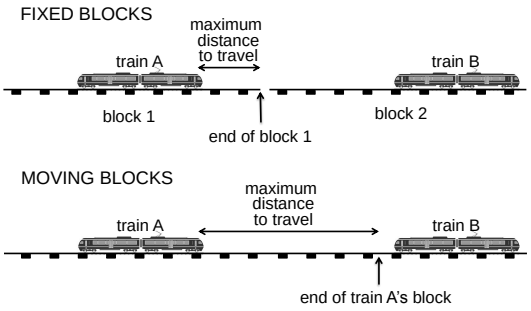

Figure 1: Fixed-block and moving-block operation.

1 Introduction

In order to avoid collisions between consecutive trains traveling on the same track, the track is traditionally divided in fixed sections—called blocks—and only one train at a time is allowed to be in a given block. Different signaling mechanisms (trackside traffic lights, communication through the track circuits, ...) are used to inform a train's driver of the presence of another train in the block ahead, so that he/she can stop the train. Automatic train protection mechanisms can intervene in case the driver fails to react. The cost of the required trackside equipment limits blocks' granularity and determines a lower bound for the trains' headway, i.e. the minimum distance (or time) achievable between two consecutive trains. The minimum headway determines the maximum line capacity, e.g. expressed in number of passengers per hour.

The increasing demand for efficient mass transit transport requires to utilize train lines more efficiently. The improvements of train-sidetrack wireless communications, on board processing and actuators have made possible the introduction in the last 15 years of moving block systems, where blocks are dynamically calculated. Figure 1 schematically illustrates the two different approaches. The moving-block control can reduce the headway taking into account the actual distance between the trains as well as their speeds. It is being deployed as Communication-Based Train Control (CBTC) for urban mass transit system and is under consideration for next generation of European Train Control System (ETCS level 3 under standardization).

In moving-block systems an on board local controller, called the Carborne Controller (CC), continuously collects and processes data about different quantities of interest like the train's position, its speed, etc. This information is sent periodically to an external ground controller, which is called the Zone Controller (ZC) because it monitors all the trains in a given zone. On the basis of the information collected from all the trains, the ZC computes the Limit of Movement Authority (LMA) for each train and sends it to the corresponding CC, using standard or proprietary radio technologies. Messages can be sent redundantly through multiple independent channels to reduce the risk that the information is lost, nevertheless such event can always occur. Given that ZC messages carry movement authorities that are safety-critical, if no LMA message is received during a given interval then the CC will no longer have valid guarantees that train movement is still safe and will trigger an Emergency Brake (EB). It is clearly desirable to limit the frequency of spurious emergency brakes, i.e. emergency brakes that are simply due to losses on the wireless channel and not to a potential collision risk. Indeed spurious emergency brake can be themselves a cause of danger, with trains potentially blocked in tunnels, risks of passengers disembarking on the tracks, etc. Moreover, a spurious EB can generate legitimate EBs on the following trains on the track, causing in this way major service disturbance. For this reason, the

so-called performance based contracts (similar to service level agreements for network operators) can bind rail transport companies to specify the maximum number of spurious emergency brakes over a given period of time.

In spite of their criticality, the estimation of the rate of spurious EBs is mostly based on historical operational data. This approach strongly limits the possibility to evaluate ahead of time the performance when significant changes are deployed and in particular when new lines based on new technologies are built. It is often required to experimentally adapt different system parameters (e.g. transmission power levels, timer values, ...) after the deployment of the line, and sometimes even to deploy additional trackside equipment (e.g. radio transmitters). These difficulties are often considered one of the reasons for the delay in the standardization of ETCS level 3. For example [12] shows that the official quality of service specifications for the different subcomponents of the ETCS level 3 system can lead to a ridiculously high rate of spurious EBs (one every 30 minutes).

A model-based analysis can then play a fundamental role for a preliminary evaluation of the real performance of moving block control. Some work has been done in this direction following [12], and then considering its abstraction from ETCS level 3 specifications mostly using stochastic Petri nets [13, 5, 1, 4, 2]. A detailed overview of the related papers is in Sec. 5, here we simply mention the four main differences of our approach. First, rather than moving from the current proposals for ETCS level 3, we consider as reference an actual implementation of the moving-block system for metro by Alstom, one of the world largest company in the domain of rail transport and signaling. This fact has important consequences on the modeling phase. One example illustrates the difference in viewpoints. ETCS level 3 specifications require loss of communication to be spaced by 7 seconds on average and to last less than 1 s in 95% of the cases. From these requirements [12] (and then the follow-ups) models the wireless channel as an ON-OFF renewal process (independent from the train movement) whose rates are determined so to match the requirements. On the contrary we explicitly consider the handover phases that are the cause of such long losses of communications and we then study them jointly with the train mobility. In fact disassociation time instants are obviously dependent on the relative position of train's and trackside's transmitters. Second, looking at an actual implementation has lead us to identify the importance of the time-slotted operation of the two controllers (the CC and the ZC). Indeed, the most important delay component in the messages' exchange between the CC and the ZC is due to the waiting time for the next clock tick at which the controller can process the message. This waiting time can be equal to hundreds of milliseconds versus the tens of milliseconds due to network delays. This aspect was ignored in the previous literature and we show that has to be addressed to correctly evaluate the system performance. In particular, a consequence of the time-slotted operation is that the EB rate exhibits non-trivial discontinuity as the timer value changes. A third (methodological) difference in comparison to the direction of [12] and follow-ups is that we try to push as further as possible the probabilistic analysis to derive closed-formula expressions. We manage to derive a formula for the case of independent and homogeneous packet losses. The analysis allows to better understand the role of the different system parameters and it is also the foundation on which we develop an efficient perfect simulation approach for the more general case. On the contrary the existing literature only relies on simulations or (in the case of [2]) on the numerical solution of a stochastic Petri net. In both cases the dependence on the system parameters is hidden. Finally, from the algorithmic point of view, it is not clear if the numerical approaches proposed until now can be practically used to estimate EB rates as low as in this paper. Our guess is that this is probably not the case but, perhaps, for [13] and [2] (see the detailed discussion in Sec. 5). Indeed our approach does not need to simulate rare sequences of packet losses and is then practically implementable (less than 1 minute on standard PCs). Our numerical approach is also validated by discrete-event simula-

tions through an ad-hoc simulator and ns-3 [10], for which we had to develop some additional modules.

Summarizing, our main contributions in this paper are the following:

1. we study moving block control starting from a real implementation,
2. we derive a simple formula for the rate of spurious EBs in the case of independent packet losses,
3. we provide an efficient Monte Carlo method to evaluate the EB rate in presence of handovers,
4. we present some new additional modules for ns-3 to simulate train-trackside communications and in particular the moving block control.

The paper is organized as follows. In Sec. 2 we describe our assumptions about the train scenario and the details of the moving-block control including typical values for system parameters. Then in Sec. 3 we describe our general approach to study the system, we show that a worst case analysis is of limited utility (Sec. 3.1.2) and then move to derive a general formula for the EB rate (Sec. 3.1.3) that requires to characterize system delays (Sec. 3.2) and losses (Sec. 3.3). Some numerical experiments are in Sec. 4. Section 5 reviews the related work and Sec. 6 concludes the paper. The acronyms used throughout are listed in Appendix A.

2 Scenario

Here we describe the specific railway scenario we consider. In our description we will refer to transmission technologies and parameters typical of a urban rail network (and then of a CBTC system), but our following analysis does not depend on these specific implementation details. What is instead required is that the random variables (r.v.s) defined below (train speed, distances between access points, etc.) have bounded support and are lower bounded by a positive constant. For a given r.v. α, we denote by $\alpha_{\min} > 0$ its lower bound and by $\alpha_{\max} < \infty$ its upper bound.[1]

We consider a train of length L moving on an infinitely long track, its speed $\nu(t)$ is a stationary process. While we allow the speed to change (differently from most of the works in the domain that implicitly assume a constant speed), we require that its variations are small on the timescale of the timer used by the moving-block control (TM defined later), i.e. over an interval of a few seconds. Typical values for the bounds of the values assumed by $\nu(t)$ as well as for the r.v.s defined later are in Table 1.

The train has two WiFi On Board Modems (OBMs) with directive antennas: one is located at the front of the train, the other at the back. We refer to them respectively as the blue and the red OBMs. Along the track there are pairs of closely-located WiFi Access Points (APs), using the same channel. The pair is called a Trackside Radio Equipment (TRE). Each AP in a TRE is devoted to communicate with one of the two OBMs and is connected to an independent wired network through which the Zone Controller (ZC) can be reached. We also label the APs, the wireless channels and the wired networks blue or red as the corresponding OBM. Hence communications between the train and the ZC are possible through separate paths, each with a single wireless link. A frequency reuse plan limits interference from other APs. The track part between two consecutive pairs of APs is called a *line segment*. Let ξ_k denote the length of the

[1] Please note that in our paper Greek letters are reserved to denote random variables and capital letters to denote system parameters.

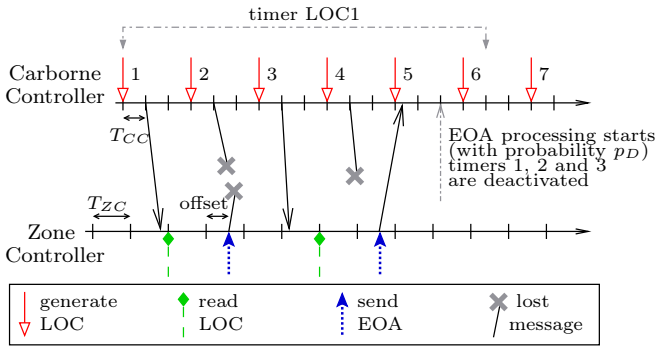

Figure 2: Illustration of LOC-EOA exchanges.

line segment between the k-th and the $k+1$-st pair of APs. We assume ξ_k to be independent samples from a random variable ξ.[2]

An OBM, say the blue one, disassociates from the blue AP it is connected to when the received signal strength falls below the given threshold. Due to the vagaries of the wireless channels, different antenna gains for different APs, and different antenna gains for the same OBM for different channels, the distance between the OBM and the AP at the disassociation is a random variable. We consider disassociation distances for different APs (of the same or of different color) to be i.i.d. r.v.s.. In particular disassociation distances from blue (resp. red) APs are samples of the r.v. δ_b (resp. δ_r). The distribution of δ_b and δ_r are in general different because of the different gain antennas have in the two opposite directions (the main antenna lobe is oriented outward). The power design guarantees that the OBM will then connect to the next blue AP along the track, i.e. to an AP that is separated by one line segment from the previous one.

2.1 Train Moving-Block Control

In this section we describe the detailed operation of a moving block system considering as reference the specific CBTC implementation by Alstom, one of the world largest company in the train transport and signaling domain.[3]

Figure 2 shows a typical messages' exchange between the on board controller (the CC) and the ground controller (the ZC). Observe that both the controllers operate in discrete time on the basis of clock periods of hundreds of milliseconds. This is due to the fact that they are actually e-out-of-f voting systems where different processors perform in parallel the same calculations and a time-slotted operation simplifies the synchronism of the processors. The clock periods at the ZC and at the CC (respectively T_{ZC} and T_{CC}) are in general different because the subsystems are provided by different vendors and also because they have different computational loads during one period.

The most important CBTC messages are location reports (LOC) and end-of-authority ones (EOA). A LOC is a message periodically transmitted from the on board Carborne Controller (CC) through the Data Communication Sub-System (DCS) to the ground Zone Controller (ZC).

[2] The analysis can be immediately extended to the case when the lengths are drawn from a distribution associated to the state of an underlying stationary Markov chain.

[3] The parameters' values have been slightly changed and some specific implementation details are hidden to protect Alstom know-how.

The message is actually sent twice through the blue and the red networks. The first LOC arriving at the ZC is processed. Each LOC is acknowledged by an EOA message in the reverse direction (again sent through the two networks). The EOA carries the LMA that indicates to the CC how far the train can advance. The LOC has a validity duration TM and a timer with such duration is activated at the generation of the LOC. An EOA is said to be valid if the timer of the corresponding LOC has not expired yet. The CC-ZC-CC exchange works as follows:

1. a LOC is generated at the CC every T_{LOC}, multiple of the CC clock period T_{CC},
2. the LOC (say LOC k) is ready to be emitted and passed to the DCS after a processing delay equal to T_{CC} since its generation,
3. the delivery delay introduced by the DCS is a random variable χ_1 with support in $[T_{DCS,\min}, T_{DCS,\max}]$,
4. at the ZC the LOC is available for computing at the next tick of the local clock,
5. the computing time at the ZC required to process the LOCs from all the trains in the zone and generate the corresponding EOAs is T_{ZC},
6. the EOA k is emitted within the next cycle of the ZC at an offset O depending on the train (the ZC sends sequentially the EOAs to all the trains in the zone),
7. the EOA is delivered to the CC after a random delay χ_2, distributed as χ_1, but independent from it,
8. at the CC the EOA gets in a processing queue, at the next tick of the CC clock the most recent EOA present in the queue is processed unless there are higher priority tasks arrived during the same CC clock period (which happens with probability p_D). In any case an EOA processing is not delayed more than an additional CC period.
9. the EOA k is actually processed only if it remains valid until the end of the current CC clock. Once processing starts, all the pending timers for older LOCs (i.e. LOC h for $h \leq k$) are deactivated.
10. if the timer of a LOC is not deactivated before its expiration, the EB procedure is triggered.

Remark We observe that the timer value TM is always large enough for an EOA to deactivate the timer of the corresponding LOC in absence of losses. If it were not the case, then spurious EBs would be systematically generated by network delays even in absence of losses.

3 Analysis

There are different metrics which could be considered to assess the emergency brakes' events. For example, one could imagine the system to be initialized at time 0 according to some specific state distribution and calculate the time distribution until the first occurrence of an emergency brake. In this paper we rather consider that the system is described by a stationary stochastic process and calculate the rate at which emergency brakes occur (considering the steady state is common to all the related literature but [2]). In particular we consider that the train is moving according to some stationary mobility model and the algorithm described above is running all the time, even after the occurrence of an emergency brake. This has some important consequences for the definition of which events are emergency brakes. If $n > 1$ consecutive LOCs experience a timeout, they should not be counted as n distinct emergency brakes events. In fact, in reality the train would stop for a while at the first timeout before starting moving again. While we find convenient analytically to imagine that the train keeps moving and the algorithm running, a sequence of multiple consecutive timeouts should only represent a single emergency brake. For this reason, a timeout for a given LOC, say LOC 1, is counted as an emergency brake only if the previous LOC 0 does not experience a timeout. LOC 0 does not experience a timeout if and

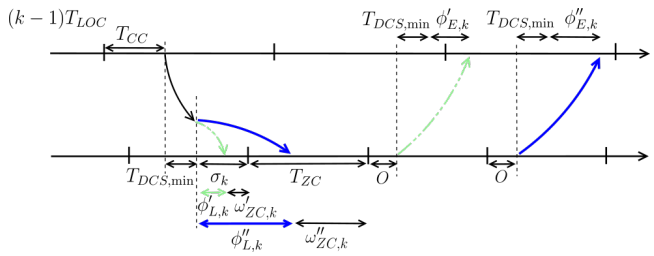

Figure 3: Different delay components of the k-th LOC-EOA exchange for two different values of the LOC transmission delay $\phi'_{L,k}$ and $\phi''_{L,k}$.

only if the corresponding LOC-EOA exchange is not lost. In fact, observe that if the exchange is not lost, then the EOA 0 will necessarily arrive in time to block the timer activated at the generation of LOC 0 (see the remark at the end of Sec. 2.1). The reverse is also true because if the exchange 0 is lost, no following EOA can block the timer of LOC 0, because they do not block the timer of LOC 1 that expires later. We denote $\mathcal{L}_k$ the event that the exchange k is lost, $\mathcal{T}_k$ the event that the k-th LOC experiences a timeout and $\bar{A}$ the complement of set A. The probability q_{EB} that a random LOC experiences an emergency break is:

$$q_{EB} = \Pr(\bar{\mathcal{L}}_0 \cap \mathcal{T}_1),$$

that does not depend on the specific pair of LOCs considered because the process is stationary. The rate of emergency brakes is then

$$r_{EB} = \frac{q_{EB}}{T_{LOC}}. \tag{1}$$

3.1 EB Probability

As we have seen in the previous section, our target is to evaluate the emergency brake probability q_{EB} for a random LOC. In this section we first derive some simple bounds for q_{EB}. The bounds will reveal to be too loose to be practically used, but they are nevertheless useful for the following analysis. We conclude the section with a general formula for the EB rate, whose terms will be calculated in the following sections. We report numerical values corresponding to the typical scenario presented in Sec. 2.

3.1.1 Minimum and maximum LOC-EOA round trip times

We calculate the minimum and the maximum time between the generation of a LOC and the instant T when the corresponding EOA is available for computation at the CC. Consider a LOC generated at time 0. Its EOA arrives at the CC at time:

$$\begin{aligned} T &= T_{CC} + T_{DCS,\min} + \phi_L + \omega_{ZC} + T_{ZC} + O + T_{DCS,\min} + \phi_E \\ &= T_{\min} + \phi_L + \phi_E + \omega_{ZC} + O, \end{aligned} \tag{2}$$

where $T_{min} = T_{CC} + 2T_{DCS,\min} + T_{ZC} = 623$ ms, ω_{ZC} is the time interval between the arrival of the LOC at the ZC and then next ZC tick and ϕ_L and ϕ_E are the random components of the transmission delays respectively for the first LOC and the first EOA to arrive at destination (see also Fig. 3).

The earliest arrival time $T_{\min}+O$ occurs when the LOC and the EOA experience the minimum travel times on the DCS (i.e. $\phi_L = \phi_E = 0$) and the LOC is available for computing at the ZC immediately before a ZC tick (i.e. $\omega_{ZC} = 0$).

The latest arrival time $T_{\max}+O$ occurs when the LOC and the EOA experience the maximum travel time on the DCS (i.e. $\phi_L = \phi_E = T_{DCS,\max} - T_{DCS,\min}$) and the LOC is available for computing at the ZC immediately after a ZC tick. In this case the LOC will wait an additional T_{ZC} before being processed (i.e. $\omega_{ZC} = T_{ZC}$). It holds:

$$T_{\max} = T_{CC} + T_{DCS,\max} + T_{ZC} + T_{ZC} + T_{DCS,\max} = 1081\text{ms}.$$

3.1.2 Number of potential LOC-EOA exchanges before a TimeOut

Even if a LOC or an EOA is lost, the EOAs corresponding to following LOCs could still deactivate its timer and then the emergency brake would be prevented. In this section we calculate how many LOC-EOA exchanges can happen between the generation of a LOC and the expiration of the corresponding timer, i.e. how many other EOAs can have a chance to block the timer.

Let consider that the first LOC is generated at time $t = 0$, then its timer would expire at time $t = TM$.

The maximum number $n_{\max}$ of LOC-EOA exchanges can be calculated considering that i) the last potentially useful EOA arrives in the shortest time possible and ii) it is immediately processed by the following CC tick, which is the last one before the timer expires. The last potential useful EOA arrives at $(n_{\max}-1)T_{LOC} + T_{\min} + O$ and it can then be processed at $T_{CC}\left\lceil \left((n_{\max}-1)T_{LOC} + T_{\min} + O\right)/T_{CC}\right\rceil$. The CC tick just before the timer expires occurs at time $T_{CC}\lfloor TM/T_{CC}\rfloor$. We determine $n_{\max}$ by imposing that:[4]

$$\left\lceil \frac{(n_{\max}-1)T_{LOC} + T_{\min} + O}{T_{CC}} \right\rceil \leq \left\lfloor \frac{TM}{T_{CC}} \right\rfloor, \tag{3}$$

and we can manipulate this inequality as in Appendix B, to obtain:

$$n_{\max} = 1 + \left\lfloor \frac{TM - \left\lceil \frac{T_{\min}+O}{T_{CC}} \right\rceil T_{CC}}{T_{LOC}} \right\rfloor. \tag{4}$$

Similarly the minimum number $n_{\min}$ of LOC-EOA exchanges can be calculated considering that i) the last potentially useful EOA arrives in the longest time possible and ii) it is processed 2 CC ticks after in correspondence of the last tick before the timer expires. Then we determine $n_{\min}$ by imposing that:

$$\left\lceil \frac{(n_{\min}-1)T_{LOC} + T_{\max} + O}{T_{CC}} \right\rceil \leq \left\lfloor \frac{TM}{T_{CC}} \right\rfloor - 1, \tag{5}$$

and proceeding as above we obtain:

$$n_{\min} = 1 + \left\lfloor \frac{TM - \left(\left\lceil \frac{T_{\max}+O}{T_{CC}} \right\rceil + 1 \right) T_{CC}}{T_{LOC}} \right\rfloor. \tag{6}$$

[4] This is correct if $n_{max} > 1$. The first EOA needs to be valid until the end of the CC clock during which it is processed and then its processing time should start the latest at the tick number $\left\lfloor \frac{TM - T_{CC}}{T_{CC}} \right\rfloor$.

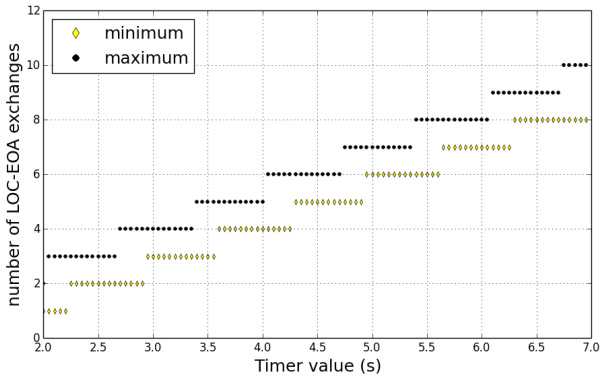

Figure 4: Minimum and maximum number of LOC-EOA exchanges for $O = 50$ ms, calculated through Eqs. (6) and (4).

The difference between $n_{\max}$ and $n_{\min}$ depends on the timer TM and also on the offset. For the typical values in Table 1 they differ by at most 2 exchanges, i.e. $n_{\max} \leq n_{\min} + 2$. Figure 4 shows the $n_{\min}$ and $n_{\max}$ for different values of the timer TM and an offset $O = 50$ ms. It also shows that the maximum difference is achieved for some values of TM.

The two values $n_{\min}$ and $n_{\max}$ allow us to provide respectively upper and lower bounds for the TM probability and then for the EB rate. In particular, let us assume that packet losses on the two wireless channels are independent Bernoulli random variables with parameter p. The probability $\tilde{p}$ to lose a LOC-EOA exchange is then $\tilde{p} = 1 - (1-p^2)^2$, because either the LOC is lost (and then no EOA will be generated) or the LOC is received but the corresponding EOA is lost.

An emergency brake requires that the exchange 0 is not lost. Moreover the EB will necessarily occur if the $n_{\max}$ following LOC-EOA exchanges are lost (even if the $n_{\max} + 1$ EOA arrives, it will be after the timer expiration) and cannot occur unless $n_{\min}$ exchanges are lost (the first $n_{\min}$ EOA cannot arrive late even in the worst case). It follows that

$$(1-\tilde{p})\tilde{p}^{n_{\max}} \leq q_{EB} \leq (1-\tilde{p})\tilde{p}^{n_{\min}}. \tag{7}$$

The upper bound can be up to $\tilde{p}^{-2}$ times larger than the lower bound. A typical value for the packet loss probability is $p = 5\%$, and then $\tilde{p} \approx 0.5\%$ and the ratio of the two bounds is almost 4×10^4. In this case, as we are going to show later, the upper bound can be too pessimistic and practically of no utility to set the parameter TM. For this reason a more refined analysis is required.

3.1.3 Exact Formula

Let consider that the LOC 1 is generated at time $t = 0$ and we number all the LOCs, so that LOC k-th is the LOC generated at $(k-1)T_{LOC}$. The k-th EOA is the EOA corresponding to the k-th LOC. The timer of LOC 1 would expire at time $t = TM$. Remember that $\mathcal{L}_k$ denotes the event that the k-th LOC-EOA exchange is lost. Let $\mathcal{D}_k$ denote the event that the k-th EOA arrives too late to deactivate the timer of LOC 1.

We assume that EOAs cannot arrive out of order at the ZC. A consequence is that:

$$\mathcal{D}_k \subset \mathcal{D}_{k'} \cup \mathcal{L}_{k'} \quad \forall k' \geq k, \tag{8}$$

in fact if the k-th EOA arrives late, a later one either does not arrive or it arrives late.

This simple relation allows us to conclude that for any m

$$\bigcap_{k=1}^{m}(\mathcal{L}_k \cup \mathcal{D}_k) = \bigcup_{k=1}^{m}\left(\mathcal{D}_k \cap \left(\bigcap_{h=1}^{k-1}\mathcal{L}_h\right)\right) \cup \left(\bigcap_{h=1}^{m}\mathcal{L}_h\right). \tag{9}$$

We prove Eq. (9) by induction in Appendix C.

The LOC 1 experiences a timeout if all the $n_{\max}$ LOC-EOA exchanges are lost or the corresponding EOAs arrive too late. We can now move to calculate q_{EB} as follows:

$$\begin{aligned}
q_{EB} &= \Pr\left(\bar{\mathcal{L}}_0 \cap \mathcal{T}_1\right) = \Pr\left(\bar{\mathcal{L}}_0 \cap \bigcap_{k=1}^{n_{\max}}(\mathcal{L}_k \cup \mathcal{D}_k)\right) \\
&= \Pr\left(\bar{\mathcal{L}}_0 \cap \left(\bigcup_{k=1}^{n_{\max}}\left(\mathcal{D}_k \cap \left(\bigcap_{h=1}^{k-1}\mathcal{L}_h\right)\right) \cup \left(\bigcap_{h=1}^{n_{\max}}\mathcal{L}_h\right)\right)\right) && (10)\\
&= \Pr\left(\bar{\mathcal{L}}_0 \cap \left(\bigcup_{k=n_{\min}+1}^{n_{\max}}\left(\mathcal{D}_k \cap \left(\bigcap_{h=1}^{k-1}\mathcal{L}_h\right)\right) \cup \left(\bigcap_{h=1}^{n_{\max}}\mathcal{L}_h\right)\right)\right) && (11)\\
&= \sum_{k=n_{\min}+1}^{n_{\max}} \Pr\left(\mathcal{D}_k \cap \left(\bar{\mathcal{L}}_0 \cap \bigcap_{h=1}^{k-1}\mathcal{L}_h\right)\right) + \Pr\left(\bar{\mathcal{L}}_0 \cap \bigcap_{h=1}^{n_{\max}}\mathcal{L}_h\right) && (12)\\
&= \sum_{k=n_{\min}+1}^{n_{\max}} \Pr\left(\mathcal{D}_k \,\middle|\, \bar{\mathcal{L}}_0 \cap \bigcap_{h=1}^{k-1}\mathcal{L}_h \cap \bar{\mathcal{L}}_k\right) \Pr\left(\bar{\mathcal{L}}_0 \cap \bigcap_{h=1}^{k-1}\mathcal{L}_h \cap \bar{\mathcal{L}}_k\right) \\
&\qquad + \Pr\left(\bar{\mathcal{L}}_0 \cap \bigcap_{h=1}^{n_{\max}}\mathcal{L}_h\right). && (13)
\end{aligned}$$

Equation (10) is obtained considering equality (9). Equation (11) follows from $\Pr(\mathcal{D}_k) = 0$ for $k \leq n_{\min}$. It can be read as follows: there is a timeout if there is a sequence of $n_{\min}$, $n_{\min}+1$ up to $\ldots n_{\max}-1$ exchanges lost and the following EOA arrives late or if all the $n_{\max}$ exchanges are lost. These events are disjoint, because $\mathcal{D}_k \cap \mathcal{L}_k = 0$, and then we can conclude Eq. (12). As observed, for the typical values in Table 1 it is $n_{\max} \leq n_{\min}+2$ and then there are at most 3 terms in Eq. (12). The final expression is Eq. (13). The reason why we introduce the additional set $\bar{\mathcal{L}}_k$ in the intersection will be clear in the following sections, where we will move to characterize delays and losses in order to compute the terms appearing in Eq. (13). Because we will need often to condition on this sequence of loss events, we denote it simply as $S_{\mathcal{L},k} \triangleq \bar{\mathcal{L}}_0 \cap \bigcap_{h=1}^{k-1}\mathcal{L}_h \cap \bar{\mathcal{L}}_k$.

3.2 Delay

In this section we characterize the event $\mathcal{D}_k$. In particular, we are interested to evaluate the probabilities $\Pr\left(\mathcal{D}_k \mid S_{\mathcal{L},k}\right)$ appearing in Eq. (13). To this purpose we will study in detail the different components that determine if the k-th EOA arrives before or after the expiration of the timer of the first LOC.

Again, assume that LOC 1 is generated at time 0. If the k-th exchange LOC-EOA is not lost, then the arrival time of the k-th EOA is

$$\begin{aligned}
T_k &= (k-1)T_{LOC} + T_{CC} + T_{DCS,\min} + \phi_{L,k} \\
&\quad + \omega_{ZC,k} + T_{ZC} + O + T_{DCS,\min} + \phi_{E,k} \\
&= T_{\min,k} + \phi_{L,k} + \phi_{E,k} + \omega_{ZC,k},
\end{aligned} \tag{14}$$

where $T_{\min,k} = T_{CC} + 2T_{DCS,\min} + T_{ZC} + (k-1)T_{LOC} + O$ and the random variables $\omega_{ZC,k}$, $\phi_{L,k}$, $\phi_{E,k}$ represent the same quantities than in Eq. (2), but are referred to the k-th exchange

rather than to the first one. The EOA is processed at the tick

$$\gamma_k \triangleq \left\lceil \frac{T_k}{T_{CC}} \right\rceil + \omega_{CC,k}, \tag{15}$$

where $\omega_{CC,k}$ represents the processing delay at the CC expressed in number of ticks. According to the description in Sec. 2.1 $\omega_{CC,k}$ can assume value 0, if the EOA is going to be processed at the first CC tick after T_k, or value 1, if it is going to be processed at the following tick. We are going to characterize the Bernoulli r.v. $\omega_{CC,k}$ soon, for the moment we observe that the EOA arrives too late if $\gamma_k > \frac{TM}{T_{CC}}$ i.e. the EOA starts being processed after the expiration of the timeout.[5] Then, the event D_k can be expressed as follows:

$$\mathcal{D}_k = \bar{\mathcal{L}}_k \cap \left\{ \gamma_k > \frac{TM}{T_{CC}} \right\},$$

and

$$\Pr\left(\mathcal{D}_k \,\middle|\, S_{\mathcal{L},k}\right) = \Pr\left(\gamma_k > \frac{TM}{T_{CC}} \,\middle|\, S_{\mathcal{L},k}\right), \tag{16}$$

because $\bar{\mathcal{L}}_k \subset S_{\mathcal{L},k}$. In order to calculate this probability we now move to consider each source of randomness in γ_k.

Processing delay at the CC Observe that $\omega_{CC,k}$ is independent of the arrival time of the k-th EOA T_k, as well as on arrival of any other EOA. In fact the queuing delay for the k-th EOA depends only on higher-priority traffic and not on the previous EOAs (that may or not being present in the processing queue), because only the most recent EOA is processed. It follows that $\omega_{CC,k}$ is independent of the event $\cap_{h=1}^{k-1} \mathcal{L}_h$ and its conditional distribution is equal to the a priori distribution provided in Sec. 2.1, i.e. $\omega_{CC,k}$ in Eq. (16) is a Bernoulli random variable with parameter p_D. While $\omega_{CC,k}$ as introduced is defined only when the k-th exchange is not lost, we can define it for any k as an independent Bernoulli random variable with parameter p_D. It can then be interpreted as the processing delay experienced by an hypothetical EOA arriving at a given time. The distribution of $\omega_{CC,k}$ does not depend on k and is independent of $S_{\mathcal{L},k}$.

Processing delay at the ZC Going back to Eq. (14), the random variable $\omega_{ZC,k}$ is dependent on the relative position of the ticks of the two clocks but also on the value of $\phi_{L,k}$. In fact the later the LOC arrives at the ZC (the larger $\phi_{L,k}$) the less the LOC has to wait until the next ZC tick (the smaller $\omega_{ZC,k}$), unless the LOC arrives so late that it misses the first available ZC tick and needs to wait for the next one. While we cannot get rid completely of this dependence, it is simpler to reverse it. With reference to Fig. 3, we express T_k with this equivalent expression:

$$\begin{aligned} T_k &= (k-1)T_{LOC} + T_{CC} + T_{DCS,\min} + \sigma_k \\ &\quad + \mathbb{1}\left(\phi_{L,k} > \sigma_k\right) T_{ZC} + T_{ZC} + O + T_{DCS,\min} + \phi_{E,k}, \\ &= T_{\min,k} + \sigma_k + \mathbb{1}_{\phi_{L,k}>\sigma_k} T_{ZC} + \phi_{E,k} \end{aligned} \tag{17}$$

where σ_k denotes the time interval between the earliest possible instant at which the k-th LOC could be received at the ZC and the next ZC tick and $\mathbb{1}_{\phi_{L,k}>\sigma_k}$ is a Bernoulli random variable

[5] For $k = 1$ if $\gamma_1 \leq \frac{TM}{T_{CC}}$, but $\gamma_1 + 1 > \frac{TM}{T_{CC}}$ then the EOA could not be processed (because it would not be valid until the end of the CC clock period) and an EB will be triggered. We do not consider this case because the timer value is always large enough to allow an EOA to deactivate the timer of the corresponding LOC (see remark at the end of Sec. 2.1).

indicating if the random component of the communication delay will cause the LOC to miss this ZC tick and then to wait for the following one. It can be easily verified that σ_k depends on the specific LOC we are considering because the two clock periods are different. Then coherently with the idea that, in order to evaluate q_{EB}, the first LOC is chosen at random, σ_k is a random variable. Observe that the variable σ_k is independent of the loss processes and in particular of $S_{\mathcal{L},k}$. Moreover, it is independent of communication delays (i.e. of the variables $\phi_{L,k}$, $\phi_{E,k}$) and of processing delay at the ZC (i.e. of $\omega_{CC,k}$). Our next task is to determine σ_k's distribution.

Given the value $\sigma_1 = s_1$ for the first LOC, the values of the other r.v.s σ_k for $k > 1$ are unequivocally determined, let $\sigma_k = s_k$. Assuming that T_{ZC} and T_{LOC} are commensurable numbers and choosing an opportune unit so that their value can be expressed as integers, Appendix D shows that the possible values for s_k are the values s in $[0, T_{ZC})$ for which the following Diophantine equation in m and n admits integer solutions:

$$mT_{ZC} - nT_{LOC} = s - s_1. \tag{18}$$

The study of this equation in Appendix D leads to the conclusions that s_k assumes all and only the values in the set $S = \{\tilde{s} + iM,\ i = 0, 1, \dots q_{ZC} - 1\}$ where M is the greatest common divisor of T_{ZC} and T_{LOC}, $T_{ZC} = q_{ZC}M$ and $\tilde{s} = s_1 \% M$. For example for the typical values we consider ($T_{ZC} = 378$ ms, $T_{LOC} = 675$ ms) it is $M = 27$, $q_{ZC} = 14$. Moreover, the sequence s_n is periodic with period q_{ZC} and then assumes the q_{ZC} values in S only once during each period. When we consider that the first LOC is a LOC selected at random, we conclude then that the variable σ_k is a uniform random variable over the set $S = \{\tilde{s} + kM, k = 0, 1, \dots q_{ZC} - 1\}$.

If the two clocks are not periodically synchronized in order to counter-act the effect of their relative frequency-shift, then the sequence s_n is in general no more periodic. If the corresponding phase shift is a random process with independent increments and negligible changes over the timescale of the timer, it is possible to study the system in the same way simply approximating σ_k with a uniform random variable on $[0, T_{ZC})$. Equivalently, in this scenario, it is possible to consider that the variable $\omega_{ZC,k}$ in Eq. (14) has the same distribution.

Communication delays In order to completely characterize the probability in Eq. (16), we need to discuss the two random variables $\phi_{L,k}$ and $\phi_{E,k}$. Remember that $\phi_{L,k}$ is the delay experienced by the "fastest" of the two LOC packets conditional on one of them arriving at the ZC. Let $\tau_{r,L}$ denote the random component of the delay experienced by the k-th LOC packet transmitted on the red network if it is not lost (we omit for simplicity the dependence on k). We can similarly introduce $\tau_{b,L}$, $\tau_{r,E}$ and $\tau_{b,E}$. These delays are independent and identically distributed random variables with Cumulative Distribution Function (CDF) $F_\tau(t)$. In particular, under the typical values in Sec. 2.1 they have support $[0, 40]$ ms. If both transmissions are successful then $\phi_{L,k} = \min\{\tau_{r,L}, \tau_{b,L}\}$ and $F_\phi(t) = 1 - (1 - F_\tau(t))^2$, otherwise if one transmission (say the blue) is lost, it will be $\phi_{L,k} = \tau_{r,L}$ and $F_\phi(t) = F_\tau(t)$. In order to calculate the general distribution of $\phi_{L,k}$ conditional on the fact that the LOC arrives to the ZC, we need to know the probabilities of the two events: i) both LOC packets arrive at the ZC and ii) only one LOC packet arrives at the ZC. These two events are in general dependent on the previous sequence of losses, it follows that the variable $\phi_{L,k}$ is in general dependent on the event $\cap_{h=1}^{k-1} \mathcal{L}_h$ (the fact that there have been $k-1$ exchanges lost before can indicate "bad" states for both the red and the blue wireless channels and then a higher probability to lose one of the two packets for the k-th LOC). In the next section we study one case where it is possible to calculate exactly the distribution of $\phi_{L,k}$. Here, we conclude by deriving some bounds. Let $\tau_L^{(u)}$, τ' and τ'' be independent random variables with CDF $F_\tau(t)$ and $\tau_L^{(l)} = \min\{\tau', \tau''\}$. The discussion above leads us to conclude that:

$$\tau_L^{(l)} \leq_{st} \phi_{L,k} \leq_{st} \tau_L^{(u)}.$$

Note that the variables $\tau_L^{(l)}$, $\tau_L^{(u)}$ can be drawn independently from the event $S_{\mathcal{L},k}$ (in particular they are always defined, even if the k-th exchange should be lost).

Let $\tau_E^{(u)}$ (resp. $\tau_E^{(l)}$) be a r.v. distributed as $\tau_L^{(u)}$ (resp. $\tau_L^{(l)}$) and independent of $\tau_L^{(u)}$ (resp. $\tau_L^{(l)}$). Let now define the random variables $\gamma_k^{(u)}$ and $\gamma_k^{(l)}$ replacing the pair $(\phi_{L,k}, \phi_{E,k})$ in Eq. (15) respectively with $(\tau_L^{(u)}, \tau_E^{(u)})$ and with $(\tau_L^{(l)}, \tau_E^{(l)})$, i.e.

$$\gamma_k^{(u)} \triangleq \left\lceil \frac{T_{\min,k} + \sigma_k + \mathbb{1}_{\tau_L^{(u)} > \sigma_k} T_{ZC} + \tau_E^{(u)}}{T_{CC}} \right\rceil + \omega_{CC,k},$$

$$\gamma_k^{(l)} \triangleq \left\lceil \frac{T_{\min,k} + \sigma_k + \mathbb{1}_{\tau_L^{(l)} > \sigma_k} T_{ZC} + \tau_E^{(l)}}{T_{CC}} \right\rceil + \omega_{CC,k}.$$

It follows that $\gamma_k^{(l)} \leq_{st} \gamma_k \leq_{st} \gamma_k^{(u)}$ (whenever γ_k is defined, i.e. when $\bar{\mathcal{L}}_k$ happens). Moreover, observe that all the random variables appearing in the definitions of $\gamma_k^{(l)}$ and $\gamma_k^{(u)}$ are independent of the losses of LOC-EOA exchanges (and in particular from $S_{\mathcal{L},k}$) and independent of each other. Having characterized the distribution of each of these variables the distributions of $\gamma_k^{(l)}$ and $\gamma_k^{(u)}$ are completely determined. We can then introduce the events:

$$\mathcal{D}_k^{(u)} = \left\{ \gamma_k^{(u)} > \frac{TM}{T_{CC}} \right\}, \mathcal{D}_k^{(l)} = \left\{ \gamma_k^{(l)} > \frac{TM}{T_{CC}} \right\}.$$

They are both independent of $S_{\mathcal{L},k}$. It follows that

$$\Pr\left(\mathcal{D}_k^{(l)}\right) \leq \Pr\left(\mathcal{D}_k \,\middle|\, S_{\mathcal{L},k}\right) \leq \Pr\left(\mathcal{D}_k^{(u)}\right) \tag{19}$$

Using these bounds for $k = n_{\min}, \ldots n_{\max}$ in Eq. (13) we can bound the timeout probability. As we are going to show in Sec. 4, the bounds are very tight, because i) the delays τ have limited support and relatively small variance, so that there is no much difference between a single delay or the minimum of two delays (differently for example from the case of samples from a heavy-tail distribution), ii) τ and ϕ are relatively small in comparison to the other delays appearing in the formulas for γ_k, $\gamma_k^{(u)}$ and $\gamma_k^{(l)}$.

3.3 Losses

We start by considering the case when packet losses are independent and homogeneous. In this case the expression (13) for the EB probability reduces to an easy-to-calculate exact formula. We then consider the effect of handovers, which introduce strongly correlated and time-variant losses. We introduce an efficient Monte Carlo method to evaluate the terms in Eq. (13) by sampling directly from the correct system stationary distribution. The approach is similar in spirit to perfect simulations for Monte Carlo Markov Chains [8]. Interestingly, the computational cost of our numerical procedure does not depend on the loss probability value and then it can be used to quantify extremely rare events (as emergency brakes should be). We finally discuss how the same approach can be used to study other causes of packet losses as fading.

3.3.1 Independent Losses

In this section we assume that each packet can be lost independently with probability p.

In this case we do no need to rely on the bounds (19), because i) the variables $\phi_{L,k}$ and $\phi_{E,k}$ do not depend on previous losses for the other exchanges and in particular on $\cap_{h=1}^{k-1}\mathcal{L}_h$ and ii) their CDF can be easily calculated. The independence allows to write:

$$\begin{aligned}\Pr\left(\mathcal{D}_k \,\middle|\, S_{\mathcal{L},k}\right) &= \Pr\left(\mathcal{D}_k \,\middle|\, \bar{\mathcal{L}}_0 \cap \bigcap_{h=1}^{k-1}\mathcal{L}_h \cap \bar{\mathcal{L}}_k\right)\\ &= \Pr\left(\mathcal{D}_k \,\middle|\, \bar{\mathcal{L}}_k\right) = \Pr\left(\gamma_k > \frac{TM}{T_{CC}}\right) \triangleq d(k),\end{aligned} \tag{20}$$

where γ_k is a function of the independent r.v.s $\omega_{CC,k}$, σ_k (already characterized in the previous section) and $\phi_{L,k}$ and $\phi_{E,k}$, whose CDF $F_\phi(t)$can be easily derived by conditioning on the number of packets arriving at the ZC/CC:

$$\begin{aligned}F_\phi(t) &= \frac{(1-p)^2}{1-p^2}\left(1-(1-F_\tau(t))^2\right) + \frac{2(1-p)p}{1-p^2}F_\tau(t)\\ &= \frac{F_\tau(t)\left(2-F_\tau(t)(1-p)\right)}{1+p}.\end{aligned} \tag{21}$$

Our definition of $d(k)$ stresses that $\Pr(\gamma_k > TM/T_{CC})$ is a function of k, but this happens because of the constant $T_{\min,k}$, while the distributions of the r.v.s $\omega_{ZC,k}$, $\sigma_{CC,k}$, $\phi_{L,k}$ and $\phi_{E,k}$ do not depend on k.

Finally, by developing the terms $\Pr\left(\bar{\mathcal{L}}_0 \cap \cap_{h=1}^{k-1}\mathcal{L}_h \cap \bar{\mathcal{L}}_k\right)$
in Eq. (13), we obtain

$$q_{EB} = \sum_{k=n_{\min}+1}^{n_{\max}} d(k)\tilde{p}^{k-1}(1-\tilde{p})^2 + \tilde{p}^{n_{\max}}(1-\tilde{p}), \tag{22}$$

where $\tilde{p} = 1-(1-p^2)^2$ is the probability that an exchange is lost.

3.3.2 Handovers

During the handover of one OBM, say the blue one, all the packets that should be transmitted by this OBM are lost. Out of the handover phase, we assume the same independent loss model considered above. Let $\eta_b(t)$ (resp. $\eta_r(t)$) be a Bernoulli random variable denoting if the blue (resp. red) OBM experiences a handover at time t. If follows that the loss process at time t is completely characterized if we know the pair $(\eta_b(t), \eta_r(t))$. In order to calculate the EB probability it is not enough to be able to derive the distribution of $(\eta_b(t), \eta_r(t))$ at a random time t, but we need to know the joint distribution over a time interval of length roughly $(n_{\max}+1)T_{LOC} + T_{\max}$, i.e. the time needed to send the $n_{\max}+1$ exchanges appearing in Eq. (13). Unfortunately the joint distribution of the process $(\eta_b(t), \eta_r(t))$ is very hard to derive. For example the correlation of $\eta_b(t)$ and $\eta_b(t+\Delta t)$ depends on how far the train travels during the time interval Δt and on its relative position to the AP it was connected to at time t. The correlation then depends on the specific sequence of line segments' lengths as well as on the speed process $\nu(t)$. The correlation of the two variables $\eta_b(t)$ and $\eta_r(t)$ depends on the sequence of line segments too, and also on the length of the train.

We rely then on an efficient way to sample from the stationary distribution of the system in order to calculate Eq. (13) via the Monte Carlo method. The main improvement here comes from avoiding to simulate the rare packet loss events (occurring with probability p).

As usual, let us denote by 0 the generation time of LOC 1. We denote by $t_{L,i}$ (resp. $t_{E,i}$) the time at which the i-th LOC (resp. EOA) is transmitted on the wireless channel. Let $\eta_{b,i}^L \triangleq$

Algorithm 1 Monte Carlo method to generate $\mathcal{H}$ samples

1: Draw the length of the current line segment $\tilde{\xi}_0$ with PDF $sf_\xi(s)/\mathrm{E}[\xi]$
2: Draw the length of the previous two line segments ξ_{-2}, ξ_{-1} and of the following one ξ_1, all with PDF $f_\xi(s)$
3: Draw the position of the front (blue) OBM's disassociation from TRE_0 and TRE_1, all with PDF $f_{\delta_b}(s)$
4: Draw the position of the back (red) OBM's disassociation from TRE_{-2}, TRE_{-1} and TRE_0, all with PDF $f_{\delta_r}(s)$
5: Draw the position X of the head of the train at the transmission instant of the LOC 0 uniformly at random in the current line segment
6: Calculate the train head's position x_i at which the i-th LOC is transmitted by the front and back OBMs ($x_i = X + ivT_{LOC}$, for $i = 0, 1 \ldots, n_{\max}$)
7: Draw the current speed of the train $\tilde{\nu}$
8: Determine the variables $\eta^L_{b,i}$, $\eta^L_{r,i}$ by considering which LOC message is transmitted at a position at most vT_{HO} after a disassociation
9: Draw the time interval σ_0 between the generation time of LOC 0 and the first ZC tick at which LOC 0 could be processed
10: Draw the DCS delays $\phi_{L,k}$, $\tau_{E,b,k}$ and $\tau_{E,r,k}$ for $i = 0, 1 \ldots, n_{\max}$
11: Calculate the transmission instants for the i-th EOAs, for $i = 0, 1 \ldots, n_{\max}$
12: Calculate the train head's position at which the i-th EOAs are transmitted by the ZC
13: Determine the variables $\eta^E_{b,i}$, $\eta^E_{r,i}$, by considering which EOA message is transmitted at a position at most vT_{HO} after a disassociation

$\eta_b(t_{L,i})$ and $\eta^L_{r,i} \triangleq \eta_r(t_{L,i})$ denote the handover states of the two channels at the transmission instant of LOC i and we define similarly the corresponding r.v.s for the EOA, $\eta^E_{b,i}$ and $\eta^E_{r,i}$.[6] Let $\mathcal{H} = \{\eta^L_{r,i}, \eta^L_{b,i}, \eta^E_{r,i}, \eta^E_{b,i}, i = 0, 1 \ldots n_{\max}\}$ be the set of values assumed by these variables and $\bar{A}$ denote the complement of the Boolean variable A. It is easy to derive the conditional probability of a specific sequence of losses given $\mathcal{H}$ similarly to what done in the independent case in Eq. (22):

$$\begin{aligned}
\Pr\left(S_{\mathcal{L},k} \mid \mathcal{H}\right) &= \Pr\left(\bar{\mathcal{L}}_0 \cap \bigcap_{h=1}^{k-1} \mathcal{L}_h \cap \bar{\mathcal{L}}_k \mid \mathcal{H}\right) \\
&= \left(1 - p^{\bar{\eta}^L_{b,0} + \bar{\eta}^L_{r,0}}\right)\left(1 - p^{\bar{\eta}^E_{b,0} + \bar{\eta}^E_{r,0}}\right) \\
&\times \prod_{h=1}^{k-1} \left(1 - \left(1 - p^{\bar{\eta}^L_{b,h} + \bar{\eta}^L_{r,h}}\right)\left(1 - p^{\bar{\eta}^E_{b,h} + \bar{\eta}^E_{r,h}}\right)\right) \\
&\times \left(1 - p^{\bar{\eta}^L_{b,k} + \bar{\eta}^L_{r,k}}\right)\left(1 - p^{\bar{\eta}^E_{b,k} + \bar{\eta}^E_{r,k}}\right). \qquad (23)
\end{aligned}$$

Obviously the last term in Eq. (13) can be exploded in a similar way:

$$\begin{aligned}
\Pr\left(\bar{\mathcal{L}}_0 \cap \bigcap_{h=1}^{n_{\max}} \mathcal{L}_h \mid \mathcal{H}\right) &= \left(1 - p^{\bar{\eta}^L_{b,0} + \bar{\eta}^L_{r,0}}\right)\left(1 - p^{\bar{\eta}^E_{b,0} + \bar{\eta}^E_{r,0}}\right) \\
&\times \prod_{h=1}^{k-1} \left(1 - \left(1 - p^{\bar{\eta}^L_{b,h} + \bar{\eta}^L_{r,h}}\right)\left(1 - p^{\bar{\eta}^E_{b,h} + \bar{\eta}^E_{r,h}}\right)\right) \qquad (24)
\end{aligned}$$

[6] Note that, even conditioning on the first LOC being at time 0, the EOA are transmitted on the wireless channel at random time instants. Moreover here we consider that the transmission on the wireless channel is instantaneous.

We can also observe that, given the transmission instant of the k-th EOA and the handover status at this instant, the event $\mathcal{D}_k$ is independent of the losses for any other exchange, i.e.:

$$\begin{aligned}\Pr\left(\mathcal{D}_k \,\middle|\, S_{\mathcal{L},k}, \mathcal{H}, t_{E,k}\right) &= \Pr\left(\mathcal{D}_k \,\middle|\, \bar{\mathcal{L}}_k, \eta^E_{b,k}, \eta^E_{r,k}, t_{E,k}\right) \\ &= \Pr\left(\gamma_k > \frac{TM}{T_{CC}} \,\middle|\, \eta^E_{b,k}, \eta^E_{r,k}, t_{E,k}\right), \end{aligned} \tag{25}$$

where $\gamma_k = \left\lceil \frac{t_{E,k}+\phi_{E,k}}{T_{CC}} \right\rceil + \omega_{CC,k}$, and $\phi_{E,K}$ has CDF:

$$\begin{aligned}&\frac{(1-p^{\bar{\eta}^E_{b,k}})(1-p^{\bar{\eta}^E_{r,k}})}{1-p^{\eta^E_{b,k}+\eta^E_{r,k}}}\left(1-(1-F_\tau(t))^2\right) \\ &+ \frac{(1-p^{\bar{\eta}^E_{b,k}})p^{\bar{\eta}^E_{r,k}} + (1-p^{\bar{\eta}^E_{r,k}})p^{\bar{\eta}^E_{b,k}}}{1-p^{\eta^E_{b,k}+\eta^E_{r,k}}} F_\tau(t), \end{aligned} \tag{26}$$

that is the extension of Eq. (21).

Equations (23), (24) and (25) are the basis for an efficient Monte Carlo method to estimate Eq. (13). We need to

1. generate independent samples of the variables $t_{E,i}$, $\eta^L_{b,i}$, $\eta^L_{r,i}$, $\eta^E_{b,i}$ and $\eta^E_{r,i}$ for $i = 0, \dots n_{\max}$ from the system stationary distribution,
2. compute Eqs. (23), (24) and (25) for each sample and combine the terms according to Eq. (13) to obtain the value of q_{EB} given the sample
3. average the values obtained.

This algorithm can be implemented and leads to significant cost reduction in comparison to the naive approach where we would simulate also the specific loss pattern. In reality, motivated by the bounds in Eq. (19), we have implemented a simpler algorithm that uses the upper bound $\Pr(\mathcal{D}^{(u)}_k)$ rather than estimating the quantity $\Pr(\mathcal{D}_k|S_{\mathcal{L},k})$. The simplification is due to the fact that $\Pr(\mathcal{D}^{(u)}_k)$ is just a function of k, while to evaluate $\Pr(\mathcal{D}_k|S_{\mathcal{L},k})$ we need to consider $\Pr\left(\mathcal{D}_k \,\middle|\, S_{\mathcal{L},k}, \mathcal{H}, t_{E,k}\right)$ that is a function of k, $t_{E,k}$ (a continuous variable) and the two binary values $\eta^E_{b,k}$, $\eta^E_{r,k}$ as shown in Eq. (25). With this approximation (whose accuracy is justified by the reasoning at the end of Sec. 3.2 and a posteriori by the results in Sec. 4), the Monte Carlo method is simply used to evaluate the loss probability terms in Eq. (13) through Eqs. (23) and (24).

We now specify how to generate a sample of $\mathcal{H}$ from the stationary distribution, the steps are in Alg. 1 and rely in particular on the analysis in Sec. 3.2. Comments to specific steps are in Appendix E.

In the next section we show the effectiveness of this approach to calculate very small rates of spurious EBs. We also observe that, while the approach here has been detailed for the specific loss process due to handovers, it can be easily extended to other causes of loss bursts, like slow fading.

4 Numerical Experiments

In this section we first compare the results of our numerical approach described in Sec. 3.3.1 with discrete-event simulations of the system. We have used two different discrete-event simulators: an ad-hoc Python simulator we have developed by scratch and ns-3.

The scenario tested by discrete-event simulations matches that described in Sec. 2 and considered in our analysis. We should then get the same results, if it were not for the approximation of relying on the upper bound $\Pr(\mathcal{D}_k^{(u)})$ rather than estimating the exact quantity $\Pr(\mathcal{D}_k|S_{\mathcal{L},k})$. We stress again that 1) this approximation leads to conservatively overestimate the actual expected EB rate, 2) its use is not crucial for the numerical method, it can be removed at the price of a slight increase in complexity (a few more random variables should be generated). The comparison confirms the upper bound to be tight. Moreover, it allows us to contrast the computational cost of our approach and of event-driven simulations.

Before moving to describe our experiments we briefly describe the additional modules for railway simulations we have implemented for ns-3. As soon as their documentation is completed, we will make them available to the research community.

4.1 NS-3 modules

The network simulator ns-3 [10] is a GPLv2 licensed discrete-event network simulator. The current version is missing some functionalities that we need to simulate train-trackside communications. First, ns-3 considers only the omnidirectional antennas for the WiFi model even if some theoretical directional antenna models are implemented for the simulation of other wireless technologies. The gain of the transmitter/receiver antennas is a key parameter for the train system because it affects the packet loss probability and the behavior of the handover process. Second, ns-3 does not yet implement a scan mechanism of beacon signals' strength transmitted by APs operating on different channels/frequencies, which is necessary for a realistic layer-2 handover implementation. Third, ns-3 does not implement a switch object and hence, changing routes after a handover at the MAC level as done in the real implementation is tricky. Using the layer-3 routing algorithms as a workaround is not an option because the convergence to the correct path may require a few seconds causing the loss of several control messages. Fourth, there are no modules for trains and—as expected—no implementation of a moving block control system.

Therefore, we have implemented new modules in ns-3 and enhanced existing ones as follows.

3D antenna pattern models. We simulated real antennas using their 3D radiation patterns as provided by the antennas vendor [7]. We implemented a module for the trackside antenna and one for the on board antenna. Each module takes as input the corresponding data sheet of the 3D radiation pattern.

Enhancing handover. We added a multi-channel scanning mechanism and modified the related objects at Channel, Physical, and MAC level, based on the rss of the received beacons and the active probe response messages.

Fast rerouting after handovers. We have modified the static routing module and added some methods to the MAC layer objects to statically and immediately update the routing tables of the nodes affected by the association/disassociation events.

CBTC protocol and its different modules. A ZC server module and a train object that contains CC server and LOC message generator modules are implemented at the application level to simulate the CBTC protocol explained in Section 3.1.2.

4.2 Results

For constant system parameters and the support of random variables, we have considered the typical values indicated in Table 1. The results we show are for a 90m-long train. The train changes speed every 100 s, and the speed evolves according to a symmetric random walk with barriers over 100 equally spaced values between 20 m/s and 22 m/s. The line segments (ξ)

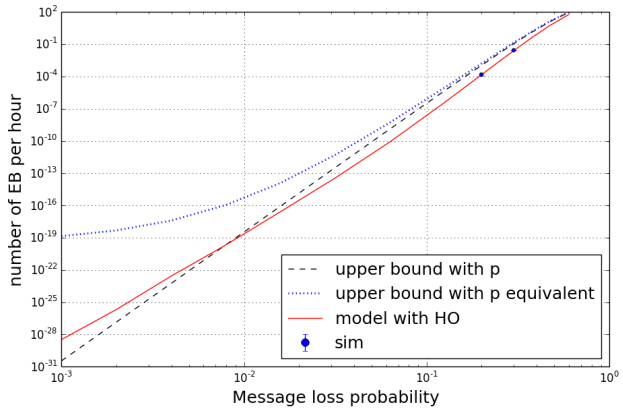

Figure 5: Number of emergency brakes per hour when $O = 50$ ms and $TO = 5.5$ s.

are uniform random variables. The disassociation distance (δ) is obtained assuming a uniform variability of AP antenna gains in a range of ± 2 dB around their nominal values.

Figures 5 and 6 show the EB rate versus different values of the packet loss probability p (out of handover phases) respectively for $TO = 5.5$ s and $TO = 2.5$ s. The red solid curves is obtained through the numerical approach described in Sec. 3.3.2. Simulation results obtained by the Python simulator for selected values of p are reported as 95% confidence intervals in blue. Our approach method relies on the upper bound $\Pr(\mathcal{D}_k^{(u)})$ and then its estimates do not need to fall inside the confidence intervals. Nevertheless, they do, but for the 3 smallest values of p in Fig. 6. The estimates are in any case very close to the results of the event-driven simulations, hence, the bound is implicitly shown to be tight. About the computational time, our numerical solver requires less than one minute to produce one point of the curve on a current commodity PC. On the same machine the Python simulator is able to simulate roughly 10^4 hours of train operation in one hour. It follows a rate of the order of 10^{-4} EBs per hour requires roughly 100 hours to be estimated with a precision of 1% through the Python simulator. It is clear that lower EB rates are out of reach for the Python simulator. The computational cost of the ns-3 simulations is even higher (60 hours are simulated in 1 hour), so that we did not manage to carry experiments for values of p smaller than 0.5. For the values we experimented, the ns-3 results are analogous to those obtained with Python and are not shown here.

Figures 5 and 6 also show some other curves. In particular the black dashed curve plots the function $(1 - \tilde{p})\tilde{p}^{n_{\min}}/T_{LOC}$, that corresponds to the upper bound in Eq. (7) in presence of independent Bernoulli packet losses with probability p. The blue dotted curve corresponds instead to a potentially more realistic way to bound the performance, considering the same Bernoulli loss model but with the actual average packet loss probability in presence of handovers p_{eq}. A simple calculation shows that $p_{eq} = \mathrm{E}[\tilde{v}]T_{HO}/\mathrm{E}[\tilde{\xi}_0] + p(1 - \mathrm{E}[\tilde{v}]T_{HO}/\mathrm{E}[\tilde{\xi}_0]) > p$. We observe that neither of the two approximations is guaranteed to lead to an upper bound for the actual system performances and even when they actually produce an upper-bound this is in general very loose. The second approximation does not lead to an upper-bound for the real system because it ignores the correlation between the red and blue handovers.

For $TO = 2.5$ s, one can be surprised to observe in Fig. 6 that the number of EBs does not vanish when p goes to zero. This is due to the fact that for $TO = 2.5$ s the number of potential LOC-EOA exchanges is 2 or 3 (see Fig. 4). When the third EOA is late, then an EB can occur

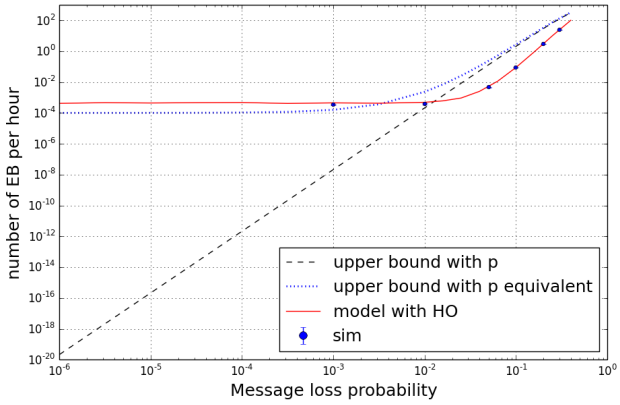

Figure 6: Number of emergency brakes per hour when $O = 50$ ms and $TO = 2.5$ s.

if the handovers cause the loss of the first two LOC-EOA exchanges. We have checked some simulation results and we have seen that this happens always according to the following scheme: the front and back handovers, the transmission of the second LOC and the transmission of the first EOA all happen very close in time (in the order of T_{HO}). In this case both the exchanges are lost and then an EB is triggered. The frequency of such event matches the results observed in Fig. 6. The presence of a horizontal asymptote for the EB rate was someway unexpected and confirms the need to pay particular attention to the effect of handovers. Similar effects can be contrasted by an accurate placement of the APs. Our analysis in this paper can be effectively used as a decision support tool to this purpose.

As a final application of our methodology, Fig. 7 shows the expected number of emergency brakes per hour for different values of the timer TM, $O = 50$ ms and packet loss probability $p = 0.05$. The theoretical values calculated from Eqs. (22) and (1) (red dots) are compared with the bounds (blue dashed lines) considering the actual packet loss probability p_{eq}. The figure shows that the simple upper bound can be orders of magnitude larger than the actual value. We now discuss the discontinuities appearing in the EB rate curve. From Eq. (22) we observe that the EB probability exhibits discontinuities only if $n_{\min}$, $n_{\max}$ or the functions $d(k)$ do. The small gaps of the EB rate correspond indeed to changes in the values $n_{\min}$ or $n_{\max}$ as it is revealed by the corresponding jumps of the bounds. The other gaps correspond to changes of the functions $d(k)$. We remember that $d(k) = \Pr(\gamma_k > TM/T_{CC})$, where γ_k is an integer. Then $d(k)$ does not depend on TM as far as $h \leq \lfloor TM/T_{CC} \rfloor < h + 1$ for some integer h. Indeed, it can be checked that the other discontinuities in the curve (when neither $n_{\min}$ nor $n_{\max}$ change) correspond to integer values of TM/T_{CC}. This high sensitivity to the timer value is not only easily revealed by our numerical method, but well explained by our theoretical analysis.

5 Related Work

The fundamental work for the quantitative evaluation of moving-block control is [12] and its extended version [13]. In these papers Zimmermann and Hommel move from probabilistic QoS specifications for the communication subsystem of ERTMS/ETCS level 3 to derive a stochastic Petri Net model for a scenario with two consecutive trains on the same track. Their objective is

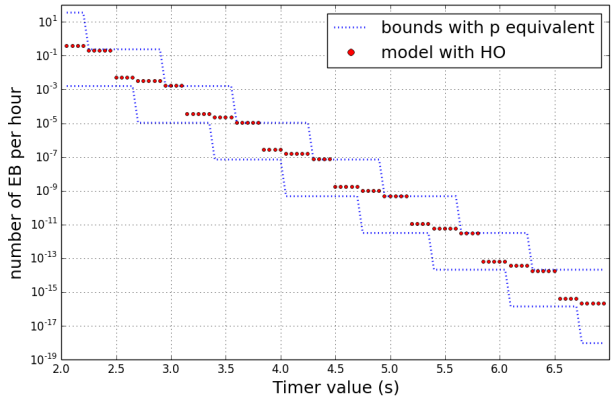

Figure 7: Rate of emergency brakes when $O = 50$ ms and $p = 0.05$.

to evaluate the EB probability. of an EB for the trailing train due to losses of LOC messages from the leading train or of EOA for the trailing train. In this case the train stops because it has no updated information about the information of the leading train. Their scenario (considered also by the following papers) is apparently more complex than ours, but in reality equivalent from the modeling point of view. The approach proposed to numerically solve the Petri Net works only under the so-called enabling restriction, i.e. only one transition can be generally distributed and all the others should be exponential r.v.s. In the more realistic cases, the authors rely then on Monte Carlo simulations of the Petri Net. The naive simulation approach presented in [12] cannot manage to quantify EB rate smaller than 2 EBs per hour. Importance splitting techniques used in [13] allow to estimate much smaller rates (about 10^{-10} per hour). It is not clear if the computational cost of this numerical approach is insensitive to the packet loss probability p as ours is.

Hermanns et al. in [5] show how the UML statechart extension called StoCharts can be used to describe the moving block control in ERTMS/ETCS level 3 and then automatically translated to MoDeST formal language (a process algebra-based formalism). Some event-driven simulation results are shown, but they fail to evaluate rare events. In a similar way Trowitzsch and Zimmermann present in [11] an approach to automatically map UML descriptions of the train system to a Stochastic Petri network.

In [1] Babczynski and Magott also use performance statecharts coupled with Monte Carlo simulations to estimate the probability of an emergency brake as a function of the timer. They consider that the number of LOC-EOA messages exchanged by the timer is $n = \lfloor TM/T_{LOC} \rfloor$ and then estimate $q_{EB} = \tilde{p}^n$ someway similarly to our bounds (7). Although their analysis ignore the difficulties of studying the two coupled discrete-time controllers, it is the first work to highlight the discontinuous dependence of q_{EB} on the timer value TM.

In the very recent paper [2] Carnevali et al. use the tool ORIS to solve numerically the Stochastic Petri net proposed in [12, 13], without the need to rely on Monte Carlo simulations. The tool indeed overcomes the limit of the enabling restriction thanks to recent advancements based on the method of stochastic state classes [6]. Moreover, it allows for a transient analysis of the system. As a case study, the authors consider a toy-example similar to that in [12] leading to very high EB rates. From a preliminary analysis using their tool, it is not clear if a more realistic scenario like the one we consider can be solved in a reasonable amount of time.

In [4], Flammini et al. evaluate the unavailability of three main systems of ERTMS/ETCS Level 2: the on board subsystem, the so-called Radio Block Centre (RBC) equivalent to the ZC in CBTC, and the communication between both through a GSM-R connection (GSM-R is an enhancement of the GSM network for railway signalling purposes). While the system they study does not use moving blocks, their conclusion is interesting for our purposes: losses on the wireless channel are the main factor determining the whole system reliability, hence the importance to develop deeper models of the train-trackside exchange. This remark is even more relevant in urban rail systems, where no regulation assigns a particular frequency to urban rail applications like CBTC and interference can be the major cause of packets losses [3].

6 Conclusion

In this paper we study the moving block control and we quantify the rate of spurious EBs. We provide analytical formulas for the simple case of independent and homogeneous packet losses, as well as a more general numerical approach with which we study the effect of losses due to handovers.

Our theoretical analysis and our numerical methods can be used as a decision support tool in order to advice on the choice of system parameters like the timer value or the spacing of APs.

7 Acknowledgments

This work is partially funded by the Inria-Alstom virtual lab.

References

[1] T. Babczyński and J. Magott. Dependability and safety analysis of ETCS communication for ERTMS level 3 using performance statecharts and analytic estimation. In *Proc. of 9th DepCoS-RELCOMEX*, volume 286 of *Advances in Intelligent Systems and Computing*, pages 37–46. 2014.

[2] L. Carnevali, F. Flammini, M. Paolieri, and E. Vicario. Non-markovian performability evaluation of ERTMS/ETCS level 3. In *Computer Performance Engineering (Proc. of EPEW 2015)*, volume 9272 of *Lecture Notes in Computer Science*, pages 47–62. 2015.

[3] P. Dersin. Availability of data communication networks in automated urban train systems. In *Proc. of RAMS 2014*, pages 1–6, Jan 2014.

[4] F. Flammini, S. Marrone, M. Iacono, N. Mazzocca, and V. Vittorini. A multiformalism modular approach to ERTMS/ETCS failure modeling. *International Journal of Reliability, Quality and Safety Engineering*, 21(1):1450001 (29 pages), 2014.

[5] H. Hermanns, D. N. Jansen, and Y. S. Usenko. From StoCharts to MoDeST: A comparative reliability analysis of train radio communications. In *Proc. of WOSP '05*, pages 13–23, 2005.

[6] A. Horváth, M. Paolieri, L. Ridi, and E. Vicario. Transient analysis of non-Markovian models using stochastic state classes. *Performance Evaluation*, 69(7-8):315–335, 2012.

[7] HUBER+SUHNER. SENCITY Spot-S WiFi antenna radiation pattern. http://www.hubersuhner.com/ProdDet/4858723.

[8] W. S. Kendall. Notes on perfect simulation. In *Markov chain Monte Carlo*, volume 7 of *IMS Lecture Notes Series*, pages 93–146. 2005.

[9] J.-Y. Le Boudec and M. Vojnovic. The random trip model: stability, stationary regime, and perfect simulation. *IEEE/ACM Transactions on Networking*, 16(6):1153–1166, 2006.

[10] ns-3 official site. https://www.nsnam.org/.

[11] J. Trowitzsch and A. Zimmermann. Using UML state machines and petri nets for the quantitative investigation of ETCS. In *Proc. of Valuetools '06*, 2006.

[12] A. Zimmermann and G. Hommel. A train control system case study in model-based real time system design. In *Proc. of IPDPS '03*, 2003.

[13] A. Zimmermann and G. Hommel. Towards modeling and evaluation of ETCS real-time communication and operation. *Journal of Systems and Software*, 77(1):47–54, 2005.

A List of Acronyms

The acronyms used in the paper are listed in Table 2.

B Deriving the Bounds of Sec. 3.1.2

$$\begin{aligned} \left\lceil \frac{(n_{\max}-1)T_{LOC}+T_{\min}+O}{T_{CC}} \right\rceil &\leq \left\lfloor \frac{TO}{T_{CC}} \right\rfloor \\ \frac{T_{LOC}}{T_{CC}}(n_{\max}-1)+\left\lceil \frac{T_{\min}+O}{T_{CC}} \right\rceil &\leq \left\lfloor \frac{TO}{T_{CC}} \right\rfloor \\ \frac{T_{LOC}}{T_{CC}}(n_{\max}-1) &\leq \left\lfloor \frac{TO}{T_{CC}} - \left\lceil \frac{T_{\min}+O}{T_{CC}} \right\rceil \right\rfloor \end{aligned} \tag{27}$$

$$n_{\max} = 1+\left\lfloor \frac{T_{CC}}{T_{LOC}} \left\lfloor \frac{TO}{T_{CC}} - \left\lceil \frac{T_{\min}+O}{T_{CC}} \right\rceil \right\rfloor \right\rfloor \tag{28}$$

$$n_{\max} = 1+\left\lfloor \frac{T_{CC}}{T_{LOC}} \left\lfloor \frac{TO-\left\lceil \frac{T_{\min}+O}{T_{CC}} \right\rceil T_{CC}}{T_{CC}} \right\rfloor \right\rfloor \tag{29}$$

$$n_{\max} = 1+\left\lfloor \frac{T_{CC}}{T_{LOC}} \frac{TO-\left\lceil \frac{T_{\min}+O}{T_{CC}} \right\rceil T_{CC}}{T_{CC}} \right\rfloor \tag{30}$$

$$n_{\max} = 1+\left\lfloor \frac{TO-\left\lceil \frac{T_{\min}+O}{T_{CC}} \right\rceil T_{CC}}{T_{LOC}} \right\rfloor \tag{31}$$

where (27) follows from T_{LOC}/T_{CC} being a natural number and (30) follows from T_{CC}/T_{LOC} being smaller than 1.

C Proof of Eq. (9)

We prove Eq. (9) by induction. It is obviously true for $m = 1$. Suppose that it is true for $m-1$, then:

$$\begin{aligned}
\bigcap_{k=1}^{m}(\mathcal{L}_k \cup \mathcal{D}_k) &= \left(\bigcap_{k=1}^{m-1}(\mathcal{L}_k \cup \mathcal{D}_k)\right) \cap (\mathcal{L}_m \cup \mathcal{D}_m) \\
&= \left(\bigcup_{k=1}^{m-1}\left(\mathcal{D}_k \cap \left(\bigcap_{h=1}^{k-1}\mathcal{L}_h\right)\right) \cup \left(\bigcap_{h=1}^{m-1}\mathcal{L}_h\right)\right) \cap (\mathcal{L}_m \cup \mathcal{D}_m) \\
&= \bigcup_{k=1}^{m-1}\left(\mathcal{D}_k \cap \left(\bigcap_{h=1}^{k-1}\mathcal{L}_h\right) \cap (\mathcal{L}_m \cup \mathcal{D}_m)\right) \\
&\quad \cup \left(\bigcap_{h=1}^{m-1}\mathcal{L}_h \cap (\mathcal{L}_m \cup \mathcal{D}_m)\right) \\
&= \bigcup_{k=1}^{m-1}\left(\mathcal{D}_k \cap \left(\bigcap_{h=1}^{k-1}\mathcal{L}_h\right)\right) \\
&\quad \cup \left(\bigcap_{h=1}^{m-1}\mathcal{L}_h \cap (\mathcal{L}_m \cup \mathcal{D}_m)\right) \qquad (32) \\
&= \bigcup_{k=1}^{m-1}\left(\mathcal{D}_k \cap \left(\bigcap_{h=1}^{k-1}\mathcal{L}_h\right)\right) \\
&\quad \cup \left(\mathcal{D}_m \cap \left(\bigcap_{h=1}^{m-1}\mathcal{L}_h\right)\right) \cup \left(\bigcap_{h=1}^{m}\mathcal{L}_h\right) \\
&= \bigcup_{k=1}^{m}\left(\mathcal{D}_k \cap \left(\bigcap_{h=1}^{k-1}\mathcal{L}_h\right)\right) \cup \left(\bigcap_{h=1}^{m}\mathcal{L}_h\right),
\end{aligned}$$

where (32) follows from Eq. (8), because $\mathcal{D}_k \cap (\mathcal{D}_m \cup \mathcal{L}_m) = \mathcal{D}_k$ for $k < m$.

D Study of the Diophantine equation (18)

Given the value $\sigma_1 = s_1$ for the first LOC, the values of the other r.v.s σ_k for $k > 1$ are unequivocally determined, let $\sigma_k = s_k$. We now study what possible values s_k can be assumed. We observe that the $n+1$-st LOC is generated at time nT_{LOC} and the earliest ZC tick at which it could be processed at the ZC is obtained by the smallest non-negative integer m^* such that $nT_{LOC} \leq s_1 + m^* T_{ZC}$. Given this value m^* the corresponding value for the s_n is $m^* T_{ZC} + s_1 - nT_{LOC}$. Assuming that T_{ZC} and T_{LOC} are commensurable numbers and choosing an opportune unit so that their value can be expressed as integers, it follows that the possible values for s_k are then the values s in $[0, T_{ZC})$ for which the following Diophantine equation in m and n admits integer solutions:

$$mT_{ZC} - nT_{LOC} = s - s_1. \qquad (33)$$

It is known that such equation admits solutions if and only if $s - s_1$ is a multiple of the greatest common divisor (g.c.d.) M of the two coefficients T_{ZC} and T_{LOC}, i.e. if and only if $s = s_1 + kM$ for $k \in \mathbb{Z}$. Moreover, we require $s \in [0, T_{ZC})$ and then only a finite number of values are possible for s. If M is the g.c.d. of T_{ZC} and T_{LOC}, then $T_{ZC} = q_{ZC} M$ and $T_{LOC} = q_{LOC} M$, with q_{ZC} and q_{LOC} prime to each other. Given that $s_0 \in [0, T_{ZC})$, it exists $\tilde{s} \in [0, M)$ and $h \in \{0, 1, \ldots q_{ZC}\}$, such that $s_1 = \tilde{s} + h \times M$. Then the possible values for s can be expressed as $s = \tilde{s} + (h+k)M$ for $k \in \mathbb{Z}$ such that $s \in [0, T_{ZC})$ or equivalently:

$$s \in S = \{\tilde{s} + kM, k = 0, 1, \ldots q_{ZC} - 1\}.$$

Then s can assume (and assume) only q_{ZC} possible values. For example for the typical values we consider ($T_{ZC} = 378$ ms, $T_{LOC} = 675$ ms) it is $M = 27$, $q_{ZC} = 42$ and $q_{LOC} = 25$.

We now observe that the values for s are periodic. In order to find the period we can look for the smallest positive integers m and n such that $mT_{ZC} + s_1 - nT_{LOC} = s_i$, i.e.

$$mT_{ZC} - nT_{LOC} = mq_{ZC}M - nq_{LOC}M = 0.$$

Given that q_{ZC} and q_{LOC} are prime to each other, by the unique factorization theorem it follows that the smallest m and n are $m = q_{LOC}$ and $n = q_{ZC}$. The values of s then repeat every $q_{LOC}q_{ZC}M$ time units or equivalently every q_{ZC} LOCs. Because the set S has q_{ZC} values and s is periodic con period q_{ZC}, it follows that s assumes all the values in S once before repeating the same sequence.

E Comments on Algorithm 1

Consider a random LOC (labeled as LOC 0). This is equivalent to considering a random observation instant of the (stationary) system. In step 1 we generate $\tilde{\xi}_0$ the length of the line segment where the head of the train is when LOC 0 is generated. The r.v. $\tilde{\xi}_0$ is stochastically larger than the length ξ of a generic line segment (this is a form of the usual inspection paradox). In order to locate the possible handovers of the front OBM occurring in a time interval of duration $(n_{\max} + 1)T_{CC} + T_{\max}$ starting from the generation of LOC 0, we need to take into account that the head of the train moves forward during this time and handovers can be experienced in following line segments. With the typical values indicated in Table 1 the head of the train cannot move farther than the following line segment, so we draw its length ξ_1 in step 2. The back OBM is located at the tail of the train, i.e. L backward than the head, so it can still be in the previous line segment. Moreover, it can be connected to a TRE located still backward (because the disassociation distance for the back OBM is longer than for the front OBM). With the typical values indicated in Table 1 and a train length $L = 90$ m, we just need to draw the lengths of the previous two line segments ξ_{-1} and ξ_{-2}. The head of the train is in the line segment of length $\tilde{\xi}_0$. Every location is equally likely, hence X is a uniform random variable in $[0, \tilde{\xi}_0]$ (step 5). We have assumed that the train speed is a stationary process, but we have not specified which one. In step 7, we assume to be able to sample from the stationary distribution of the train's speed (see for example [9] for correct sampling techniques for different synthetic mobility models). Step 8 is where we use the approximation of considering the speed constant over short timescales (order of the TM). The analysis in Sec. 3.2 allows us to correctly sample the positions of the ZC ticks in relation to the CC ticks (step 9). Note that we only generate the relative position for a single pair of ticks, because the two clocks are periodic. LOC delay can be correctly generated because the handover variables $\eta^L_{b,i}$, $\eta^L_{b,r}$ have already been calculated (the CDF of $\phi_{L,i}$ is the same as in Eq. (26) with η^E_* replaced by η^L_*). The EOA 0 transmission time on the blue channel can then be calculated (step 11) as $T_{CC} + T_{DCS,\min} + \sigma_0 + \mathbb{1}(\phi_{L,0} > \sigma_0)\, T_{ZC} + T_{ZC} + O + T_{DCS,\min} + \tau_{E,b,0}$ and analogous equation can be easily derived for the other channel and the other EOAs.

Contents

Table 1: Notation and typical values for the variables. We omit subscripts for some of the variables. A subscript b (r) denotes that the variable refers to the blue (red) OBM or network. A subscript L (E) denotes that it refers to a LOC (an EOA).

Symbol	Quantity	Value
ν	train speed	≤ 80 km/h
ξ	line segment length	$[200, 300]$ m
δ_b	disassociation distance TRE-OBM	$[100, 200]$ m
δ_r	disassociation distance TRE-OBM	$[150, 300]$ m
T_{HO}	duration of handover	100 ms
T_{ZC}	ZC clock period	378 ms
T_{CC}	CC clock period	225 ms
T_{LOC}	LOC generation period	$3T_{CC}$
TM	validity duration of a LOC	5.5 s
T_{DCS}	transmission delay	$[10, 50]$ ms
τ	positive random component of T_{DCS}	$[0, 40]$ ms
ϕ	positive random component of T_{DCS} for first message to arrive	$[0, 40]$ ms
ω_{ZC}	time interval between LOC arrival at ZC and next ZC tick	$[0, T_{ZC}]$ ms
σ	time interval between earliest LOC arrival at ZC and next ZC tick	$[0, T_{ZC}]$ ms
O	EOA transmission offset	$[0, T_{ZC}]$
ω_{CC}	number of CC ticks an EOA waits until CC processes it	$\{0, 1\}$
p_D	probability that ω_{CC} is 1	0.01
q_{EB}	emergency brake probability	
r_{EB}	emergency brake rate	
p	packet loss	
$\tilde{p}$	probability to lose a LOC-EOA exchange	
T_k	arrival time of k-th EOA	
γ_k	tick at which k-th EOA is processed	
$\mathcal{D}_k$	event that k-th EOA is late to deactivate the timer of LOC 1	
$\mathcal{T}_k$	event that k-th LOC experiences a timeout	
$\mathcal{L}_k$	event of k-th LOC-EOA exchange loss	
$\eta(t)$	Bernoulli random variable denoting if OBM experiences a handover at time t	

Table 2: List of Acronyms

AP	Access Point
CBTC	Communication Based Train Control
CC	Carborne Controller
CDF	Cumulative Distribution Function
DCS	Data Communication Sub-System
EB	Emergency Brake
EOA	End-Of-Authority
ERTMS	European Rail Traffic Management System
ETCS	European Train Control System
LMA	Limit of Movement Authority
LOC	Location report
OBM	On Board Modem
PDF	Probability Distribution Function
TM	validity duration Timer of a LOC
TRE	Trackside Radio Equipment
ZC	Zone Controller

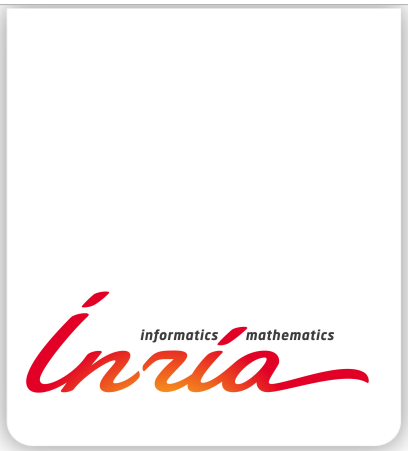

RESEARCH CENTRE
SOPHIA ANTIPOLIS – MÉDITERRANÉE

2004 route des Lucioles - BP 93
06902 Sophia Antipolis Cedex

Publisher
Inria
Domaine de Voluceau - Rocquencourt
BP 105 - 78153 Le Chesnay Cedex
inria.fr

ISSN 0249-6399